

## STRUCTURAL AND OPTICAL PROPERTIES OF LaFeO<sub>3</sub> AND La<sub>0.8</sub>Sr<sub>0.2</sub>FeO<sub>3</sub> POWDERS

Mya Theingi<sup>1</sup>, Subhajit Nandy<sup>2</sup>, Sudakar Chandran<sup>3</sup>

### Abstract

LaFeO<sub>3</sub> is one of the perovskite structure materials and its optical, electrical and magnetic properties had been frequently investigated. In the present work, nanoparticles of pure LaFeO<sub>3</sub> was prepared using the citrate sol-gel method. Sr<sup>2+</sup> ion doped LaFeO<sub>3</sub> or La<sub>0.8</sub>Sr<sub>0.2</sub>FeO<sub>3</sub> was also synthesized by the same method to study the enhancement of the structural and optical properties. The synthesis involved the sol-gel method, followed by gradual heat treatment for the combustion of organic substances. The resulting powders were characterized by several techniques such as X-Ray diffraction (XRD), scanning electron microscopy (SEM) and Raman spectroscopy to study structure, morphology and the average particle size, phase, and composition. Optical properties were investigated by using the Tauc plot methodology. The optical band gap values were evaluated by diffuse reflectance spectroscopy measurements. The calculated optical band gap were found to be 2.20 eV, 2.37 eV for x = 0.00 and 0.2, respectively. The obtained results show that the structural, morphological and optical properties have affected by the substitution of Sr<sup>2+</sup> on La<sup>3+</sup> ion in the crystal lattice of LaFeO<sub>3</sub>.

**Keywords:** La<sub>0.8</sub>Sr<sub>0.2</sub>FeO<sub>3</sub>, perovskite, citrate sol-gel method, optical properties

### Introduction

Rare-earth orthoferrites, with general formula ABO<sub>3</sub> (A = lanthanide, B = Fe) have become one of the most promising candidates due to their wide range of physical and technological properties, such as ferroelectricity, piezoelectricity, pyroelectricity, high-temperature superconductivity, magnetic behaviour, and catalytic activity (Parida *et al.*, 2010; Thirumalairajan *et al.*, 2013). LaFeO<sub>3</sub> is one of the most promising perovskite materials, which crystallizes in orthorhombic structure with space group *Pbnm*. Here the large cations La are located at the unit cell corners while the cation Fe occupies the centre of the distorted octahedron of oxygen anions of the ABO<sub>3</sub> structure where, the degree of distortion depends on the radius of the rare earth ion. The La site doping with other alkaline earth or transition metal ions is believed to be an effective way to alter the properties (Selvadurai *et al.*, 2015; Kafa *et al.*, 2017). In this regard, a variety of doped LaFeO<sub>3</sub> have been reported where doping affects the structural properties and improves its physico-chemical properties.

The easiest route for the preparation of LaFeO<sub>3</sub> is the solid-state reaction where the precursor components of metal oxides or carbonates are calcined at a temperature higher than 1273 K. But this process contains several drawbacks such as no control over the particle size, poor homogeneity and high porosity of the samples. To improve the homogeneity and also to lower the preparation temperature several wet chemical methods have been proposed by different reports which include hydrothermal synthesis, solution combustion synthesis, sol-gel, co-precipitation to obtain ultrafine pure powders (Liu *et al.*, 2016; Abdallah *et al.*, 2019).

In the present work, Sr ion is partially replacing the La ion in the crystal lattice of LaFeO<sub>3</sub> prepared by the citrate sol-gel combustion method. In addition, the structural, morphological and optical properties of the prepared nanocrystalline LaFeO<sub>3</sub> and La<sub>0.8</sub>Sr<sub>0.2</sub>FeO<sub>3</sub> powder were also investigated.

---

<sup>1</sup> Dr, Associate Professor, Department of Chemistry, Taunggoke Degree College

<sup>2</sup> PhD, Multifunctional Materials Lab, Department of Physics, Indian Institute of Technology Madras

<sup>3</sup> Associate Professor, Multifunctional Materials Lab, Department of Physics, Indian Institute of Technology Madras

## Materials and Methods

Lanthanum(III) nitrate hexahydrate ( $\text{La}(\text{NO}_3)_3 \cdot 6\text{H}_2\text{O}$ ), iron(III) nitrate nonahydrate ( $\text{Fe}(\text{NO}_3)_3 \cdot 9\text{H}_2\text{O}$ ), strontium nitrate ( $\text{Sr}(\text{NO}_3)_2$ ), citric acid monohydrate ( $\text{C}_6\text{H}_8\text{O}_7 \cdot \text{H}_2\text{O}$ ) were purchased from THE I.L.E. CO. Ltd., Chennai, India. All the reagents are SIGMA-ALDRICH brand and used as received.  $\text{LaFeO}_3$  and Sr doped  $\text{LaFeO}_3$  were synthesized from the metal-organic complexes precursor by the citrate sol-gel combustion method. In a stoichiometric ratio of La:Fe is 1:1 mol % for pure  $\text{LaFeO}_3$  and La : Sr : Fe is (4/5):(1/5):1 mol % for  $\text{La}_{0.8}\text{Sr}_{0.2}\text{FeO}_3$  and were dissolved in deionized water, and a citric acid complexing agent was added. The molar amount of citric acid was equal to a total molar amount of metal nitrates in the solution. The mixture was heated under magnetic stirring at a constant temperature of  $80^\circ\text{C}$  to form a sol, and the sol was aged at the same temperature to form a gel. The gel was first pre-calcined in a muffle furnace at  $300^\circ\text{C}$  for 5 h and then ground to a fine powder for further calcination in the furnace. These powders were ground and calcined at the temperature of  $600^\circ\text{C}$  for 5 h in the furnace to make the incompletely combusted part react thoroughly. The prepared Sr doped and undoped  $\text{LaFeO}_3$  powders were characterized and XRD, SEM, Raman spectroscopy and optical band gap measurements. Phase and structure of the prepared Sr doped and undoped  $\text{LaFeO}_3$  powders were investigated by Panalytical powder diffractometer with  $\text{CuK}\alpha_1$  radiation ( $\lambda = 1.5405 \text{ \AA}$ ). Field emission scanning electron microscope (Quanta 400, FEI microscope) was employed to observe the morphology determination, and the dispersion of particles. The Raman spectra of all samples were obtained with a 632 nm red excitation line of He-Ne laser using Horiba Jobin-Yvon (HR800 UV) micro-Raman spectrometer in the wavenumber range from 100 to  $1000 \text{ cm}^{-1}$ . Diffuse reflection spectra were obtained by Perkin Elmer 2 plus UV-Vis-NIR spectrometer for the optical properties study of the samples in the wavelength range from 300 to 1000 nm. Optical band gap of the powder samples were estimated using Tauc plots.

## Results and Discussion

X-ray diffraction patterns of Sr doped and undoped  $\text{LaFeO}_3$  are shown in Figure 1. The diffraction peaks of pure and Sr doped samples were single phase with no trace of impurities. Moreover, the (121) peak drift figure of XRD patterns demonstrated that all the samples were of perovskite orthogonal structure (PDF#37-1493) with  $Pbmn$  space group (No. 62). This volume contraction is expected because of the small difference in ionic radii of  $\text{Sr}^{2+}$  ( $1.18 \text{ \AA}$ ) and  $\text{La}^{3+}$  ( $1.36 \text{ \AA}$ ) ions.

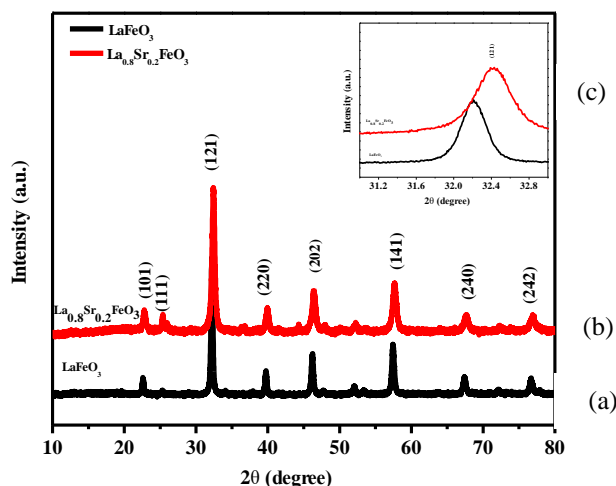


**Figure 1** X-ray diffraction patterns of (a)  $\text{LaFeO}_3$ , (b)  $\text{La}_{0.8}\text{Sr}_{0.2}\text{FeO}_3$  powder and (c) (inset) their (121) peak figures

The average crystallite sizes of samples were calculated from the dominant peaks of X-ray line broadening planes using Scherrer equation,  $D_{Sch} = \frac{0.9\lambda}{\beta \cos\theta}$ , where  $D_{Sch}$  is the average crystallite size,  $\theta$  is the Bragg angle,  $\lambda$  is the wavelength of the X-ray,  $\beta$  is the full width at half maximum, the constant  $k$  is taken as 0.9. The average crystallite sizes are summarized in Table 1. In addition, the crystallite size and the microstrain of samples were also calculated for the comparison by using the Williamson-Hall equation,  $\beta_T \cos\theta = \varepsilon (4 \sin\theta) + \frac{k\lambda}{D_{WH}}$ , where  $D_{WH}$  is the average crystallite size,  $\theta$  is the Bragg angle,  $\lambda$  is the X-ray wavelength,  $k = 0.9$ ,  $\beta$  is the full width at half maximum of XRD peaks and  $\varepsilon$  is the microstrain of the lattice (Smirnova, 1999). The plots of  $\beta \cos\theta$  as a function of  $\sin\theta$  are shown in Figure 2.  $D_{WH}$  and  $\varepsilon$  of samples are determined from the linear extrapolation and slope of these plots, respectively. All of these values are summarized in Table 1. The crystallite size of  $La_{0.8}Sr_{0.2}FeO_3$  was 29 nm for Sr doping while those of  $\varepsilon$  increased from 0.134 % to 0.246 % due to the shrinkage of the lattice parameters.

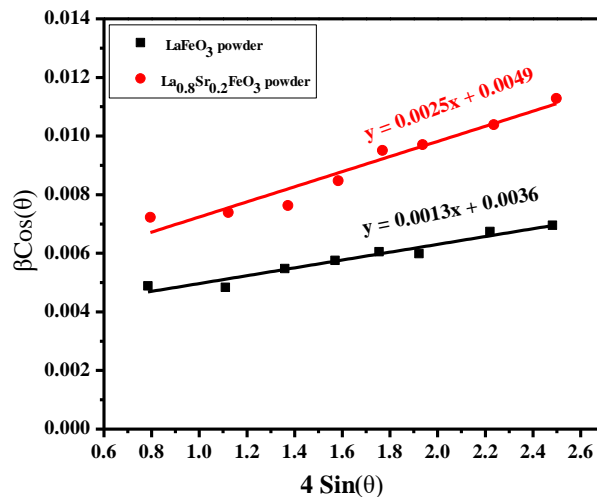


**Figure 2** Williamson-Hall plots of  $\beta \cos\theta$  against  $4\sin\theta$  calculated from XRD spectral data of  $LaFeO_3$  and  $La_{0.8}Sr_{0.2}FeO_3$  powders

**Table 1** Average Crystallite Size, Strain of the Prepared Powder Samples

Samples	Average crystallite size (nm)		Strain (%)
	Scherrer equation	Williamson-Hall Plot	
$LaFeO_3$	24	38	0.134
$La_{0.8}Sr_{0.2}FeO_3$	15	29	0.246

Figure 3 (a), and (b) show Rietveld refined XRD patterns of (a)  $LaFeO_3$  and (b)  $La_{0.8}Sr_{0.2}FeO_3$  powders that were analyzed by using Fullprof suite software. The observed Residual factors and atomic coordinates of Rietveld refinement of powders samples are listed in Table 2. All the XRD patterns were assigned to orthorhombic structure with a space group  $Pbnm$  (No.62) using CIF file. Furthermore, no other impurity phases were observed from the XRD patterns and it confirmed the single phase formation of samples observed within the detection limit of the XRD. Also, it indicated the absence of biphasic structure such as  $LaFeO_3$  and  $LaSrO_3$  in doping samples, since both the compound has distinct lattice parameters. Moreover, the peak shift to higher angle  $2\theta$  was noted on Sr substitution in  $LaFeO_3$ . This peak shifting confirms that, there are no biphasic present in the samples. Thus, reduction in the lattice parameter observed for Sr may be due to the induced defects, which enhances the physical properties of the prepared samples.

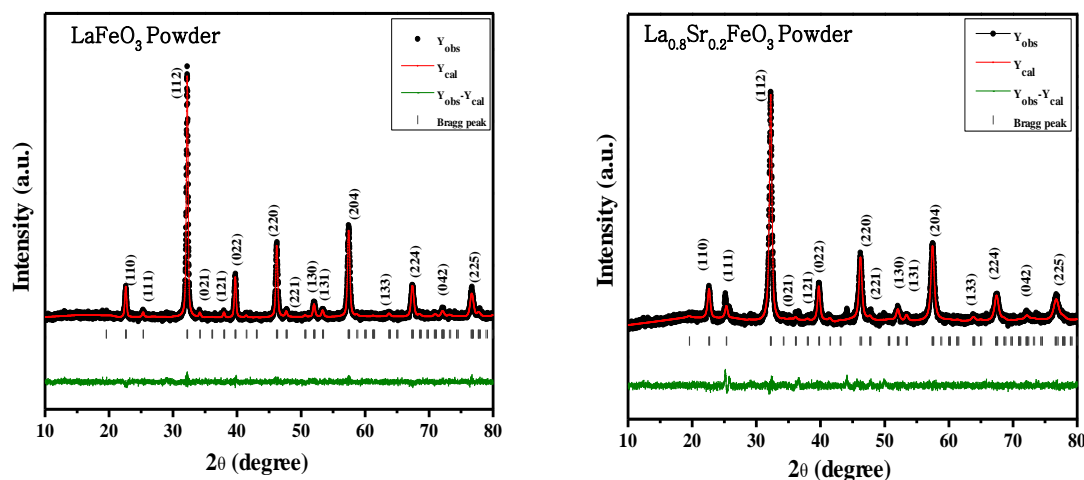


**Figure 3** Rietveld refined XRD patterns of (a)  $\text{LaFeO}_3$  and (b)  $\text{La}_{0.8}\text{Sr}_{0.2}\text{FeO}_3$  powders by Fullprof software

**Table 2** Structural Parameters and Reliability Factors obtained from Rietveld Analysis of Sr Doped and Undoped  $\text{LaFeO}_3$  Powders of XRD Patterns

Samples	Lattice Parameters ( <i>Pbnm</i> setting)				R-factors		
	a (Å)	b (Å)	c (Å)	V (Å <sup>3</sup> )	wR <sub>p</sub> (%)	R <sub>p</sub> (%)	χ <sup>2</sup>
$\text{LaFeO}_3$	5.5567	5.5618	7.8496	242.631	5.63	3.48	1.11
$\text{La}_{0.8}\text{Sr}_{0.2}\text{FeO}_3$	5.5609	5.5568	7.8388	242.231	4.62	3.52	1.46

The microstructure of the  $\text{La}_{1-x}\text{Sr}_x\text{FeO}_3$  ( $x=0$  and  $0.2$ ) powder samples was investigated using a scanning electron microscope (SEM) and the recorded SEM micrographs are shown in Figure 4. Powder samples revealed irregular particle shapes with a wide-range of particle size distribution, consisting of nanometer-sized particles and macroplate-like agglomerations. The EDX analysis was employed to determine the element of the synthesized materials. The elemental compositions of powder samples in terms of atomic weight percentages are listed in the Table 3. The elemental composition values are almost in close agreement with the stoichiometry of starting materials used for the preparation of samples.

**Table 3** Semiquantitative Chemical Compositions Present in the Powder Samples

Sample	Atomic %			
	La	Sr	Fe	O
$\text{LaFeO}_3$	17.7	-	20.1	62.2
$\text{La}_{0.8}\text{Sr}_{0.2}\text{FeO}_3$	11.1	3.5	15.3	70.2

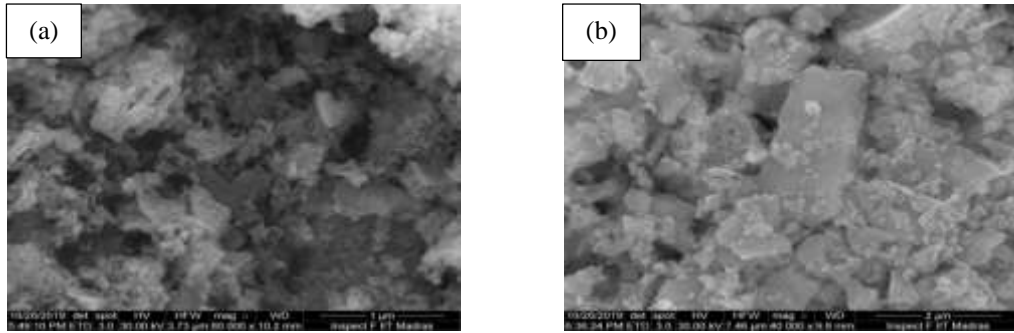


**Figure 4** SEM images of the powder samples (a)  $\text{LaFeO}_3$  and (b)  $\text{La}_{0.8}\text{Sr}_{0.2}\text{FeO}_3$

One of the advantages of Raman spectroscopy is that it has a very sensitive to structure distortion and oxygen motion. Therefore, a detailed investigation of electron excitation is very important to understand the doping effect of perovskite-type materials. Room temperature Raman spectra recorded for the prepared samples are shown in Figure 5. According to the group theory analysis that the Brillion zone center normal modes transform according to the representation:  $7A_g + 8 A_u + 5B_{1g} + 10B_{1u} + 7B_{2g} + 8B_{2u} + 5B_{3g} + 10B_{3u}$ . The representation  $A_u + 2B_u$  belongs to three acoustic modes. Modes  $A_g$ ,  $B_{1g}$ ,  $B_{2g}$  and  $B_{3g}$  are Raman active and Modes  $A_u$ ,  $B_{1u}$ ,  $B_{2g}$ ,  $B_{2u}$ ,  $B_{3g}$  and  $B_{3u}$  are infrared active (Sharma *et al.*, 2017). Raman spectra were recorded using 632 nm laser diode. The modes were measured between the regions of  $1000 \text{ cm}^{-1}$ - $100 \text{ cm}^{-1}$ . The modes between 200 and  $30 \text{ cm}^{-1}$  (denoted as A) are assigned to lattice and La vibrations due to the more mass of the La ion, modes between 350 and  $200 \text{ cm}^{-1}$  (denoted as T) are assigned to oxygen octahedral tilt modes, and modes between 450 and  $350 \text{ cm}^{-1}$  (denoted as B) are assigned as bending modes and modes above  $500 \text{ cm}^{-1}$  (denoted as S) are assigned to oxygen stretching vibrations. The spectra of  $\text{LaFeO}_3$  and Sr doped samples are distinct from each other. The broaden, appearance and disappearance of phonon modes indicate toward structural rearrangement in the system and such a deviation is considered as a sign of presence of spin-phonon coupling and mixed tendency of  $\text{Li}^{3+}$  and  $\text{Sr}^{2+}$  metal ions. No Raman mode above  $800 \text{ cm}^{-1}$  indicates the absence of impurity phase in doping.

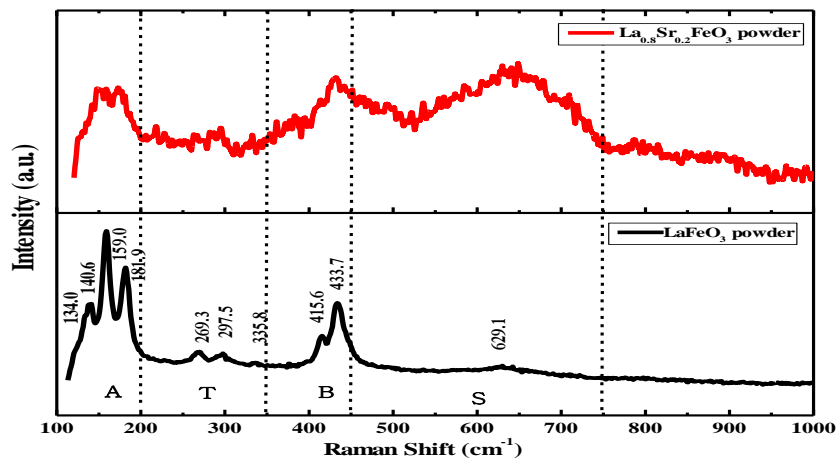


**Figure 5** Raman spectra of Sr doped and undoped calcined powders

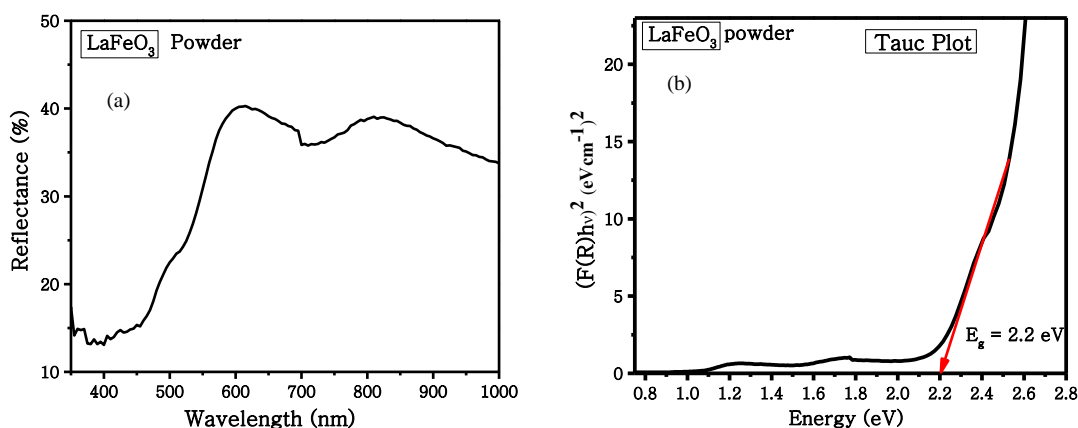


**Figure 6** (a) Diffuse reflectance spectrum (b) Plot of  $(F(R) \cdot hv)^2$  vs. the energy in electron volts of  $\text{LaFeO}_3$  powder

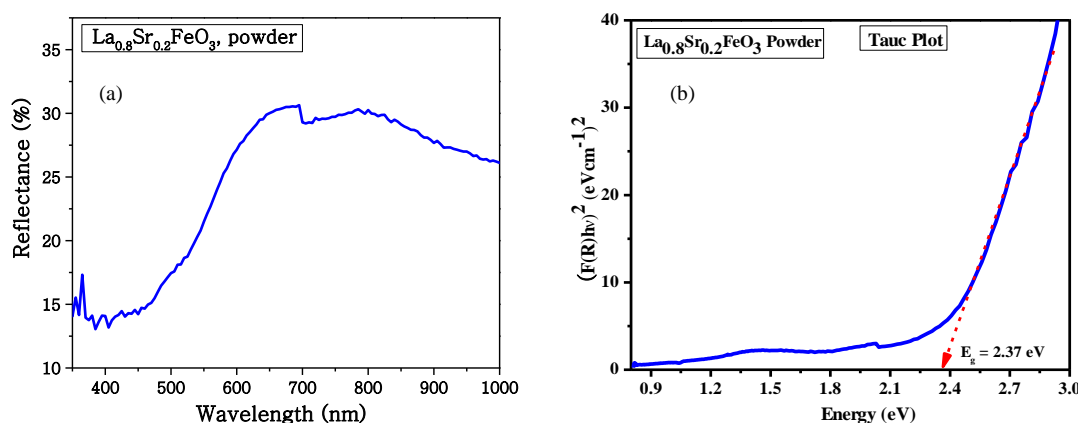


**Figure 7** (a) Diffuse reflectance spectrum (b) Plot of  $(F(R) \cdot hv)^2$  vs. the energy in electron volts of  $\text{La}_{0.8}\text{Sr}_{0.2}\text{FeO}_3$  powder

Figure 6 and 7 show the diffuse reflectance spectra and Tauc plots of pure  $\text{LaFeO}_3$ , and  $\text{La}_{0.8}\text{Sr}_{0.2}\text{FeO}_3$ , respectively, and all samples show strong visible-light absorption but by doping Sr on La site it can be seen that decreasing in visible-light absorption. Band gap energy can be determined from Kubelka-Munk equation via a Tauc plot,  $\alpha = B (hv - E_g)^n / hv$ , where  $\alpha$  is the absorption coefficient,  $\nu$  is the irradiation frequency,  $E_g$  is the band gap,  $B$  is a constant (being usually 1 for semiconductor),  $h$  is the Planck constant and  $n$  is a constant depending on the type of semiconductor (direct transition:  $n = 1/2$ ; indirect transition:  $n = 2$ ). Diffuse reflectance UV-Vis spectroscopy (DRS) can be mathematically expressed in terms of absorption coefficient through differential equations obtained from Kubelka-Munk theory. Substituting the Kubelka-Munk function ( $F(R_\infty)$ ) in the Tauc equation, the intercept of linear region of  $F(R_\infty) = B (hv - E_g)^n$  curve on the x-axis gives the value of the band gap energy of the sample.  $F(R_\infty) = \frac{(1-R_\infty)^2}{2R_\infty} = \frac{K}{S}$ ,  $R_\infty$  is diffused reflectance of the powder sample,  $K$  is effective absorption coefficient and  $S$  is scattering coefficient. The band gap energy can be determined by extrapolating the slope to  $F(R) \rightarrow 0$  (Roberto *et al.*, 2013; Schevciw and White, 1983). It is a well-known effect that small particles tend to exhibit increased band gaps and it agrees with Sr doping on  $\text{LaFeO}_3$ . The proper replacement of lanthanum by Sr ion is the best proof for the increase in the band gap energy. This confirms that  $\text{Sr}^{2+}$  ion can affect the optical transition in  $\text{La}_{0.8}\text{Sr}_{0.2}\text{FeO}_3$ .

## Conclusion

Pure LaFeO<sub>3</sub> and Sr doped La<sub>1-x</sub>Sr<sub>x</sub>FeO<sub>3</sub> (x=0.2) perovskite powders were synthesized by the citrate sol-gel combustion method. The XRD patterns confirmed the formation of single phase orthorhombic perovskite crystal structure with *Pbmn* space group for Sr doped and undoped LaFeO<sub>3</sub>. The lattice parameters of the synthesized samples were calculated by fullprof retrieved refined method. Morphology of Sr doped LaFeO<sub>3</sub> powders differed from those of the pure LaFeO<sub>3</sub>. This is because the doped ions can cause the disorderness of the atomic configuration in LaFeO<sub>3</sub>. All the powder sample showed uniform and quite good in grain distribution, with plate form of grains agglomeration in SEM images. The presence of expected elements in the prepared powders was confirmed by EDX analysis. Raman spectra determine the various functional groups present in the prepared LaFeO<sub>3</sub> and Sr doped LaFeO<sub>3</sub> powder samples. The optical band gap increased with Sr doping in the prepared powder samples. The optical band gap energy of the Sr doped LaFeO<sub>3</sub> powder is 2.37 eV whereas that of undoped LaFeO<sub>3</sub> powder is 2.20 eV. A good correlation between structural and optical properties has been observed for the studied samples. Actually, the distortion of the structure caused by doping leads to a change in optical properties. These interesting properties allow the material to be used in novel applications in the field of science and technology.

## Acknowledgements

The authors would like to thank ASEAN- India Research Training Fellowship Program (AIRTF) for providing this Fellowship. The authors express thanks to Dr Sudakar Chandran, Multifunctional Material Laboratory, for guiding in this work. The authors are also thankful to the Indian Institute of Technology Madras (IITM), and Department of Physics IITM, for all the microscopy and research facilities. The authors also would like to express their profound gratitude to the Department of Higher Education, Ministry of Education, Yangon, Myanmar, for provision of opportunity to do this research and Myanmar Academy of Arts and Science for allowing to present this paper.

## References

- Abdalah, F. B., Benali, A., Triki, M., Dhahri, E., Nomenyo, K. and Lerondel, G. (2019). "Investigation of Structural, Morphological, Optical and Electrical Properties of Double-doping Lanthanum Ferrite". *J. Mater. Sci. Materials in Electronics*, vol. 30, pp. 3349–3358
- Kafa, C.A., Triyono, D. and Laysandra, H. (2017). "Temperature-dependent Impedance Spectroscopy of La<sub>0.8</sub>Sr<sub>0.2</sub>FeO<sub>3</sub> Nano-crystalline Material". *Mater. Sci. and Eng.*, vol.188, pp. 012027, 1-5
- Liu, Q. S., You, Z., Zeng, S. J. and Guo, H. (2016). "Infrared Properties of Mg-doped LaFeO<sub>3</sub> Prepared by Sol-gel Method". *J. Sol-Gel Sci. Technol.*, vol. 80, pp. 860–866
- Parida, K.M., Reddy, K.H., Martha, S., Das, D.P. and Biswal, N. (2010). "Fabrication of Nanocrystalline LaFeO<sub>3</sub>: An Efficient Sol-gel Auto-combustion Assisted Visible Light Responsive Photocatalyst for Water Decomposition". *Int. J. Hydrogen Energy*, vol. 35, pp. 12161 - 12168
- Roberto, K., Lothar, J. and Stefan, G. E. (2013). "Magnetic and Optical Investigations on LaFeO<sub>3</sub> Powders with Different Particle Sizes and Corresponding Ceramics". *Solid State Ionics*, vol. 249–250, pp. 1-5
- Schevciw, O. and White, W. B. (1983). "The Optical Absorption Edge of Rare Earth Sesquisulfides and Alkaline Earth-Rare Earth Sulfides". *Mat. Res. Bull.*, vol.18, pp.1059-1068
- Selvadurai, A. P. B., Pazhanivelu, V., Jagadeeshwaran, C., Murugaraj, R., Muthuselvam, I. P. and Chou, F.C. (2015). "Influence of Cr Substitution on Structural, Magnetic and Electrical Conductivity Spectra of LaFeO<sub>3</sub>". *J. Alloys and Compounds*, vol. 646, pp. 924-931
- Sharma, G., Tyagi, S. and Sathe, V. G. (2017). "Raman Spectroscopic Investigation of Spin-Lattice Coupling In LaFeO<sub>3</sub>". *AIP Conference Proceedings*, vol.1832, pp. 090020, 1-2
- Smirnova, I.S. (1999). "Normal Modes of the LaMnO<sub>3</sub> Pnma Phase: Comparison with La<sub>2</sub>CuO<sub>4</sub> Cmca Phase". *Physica B*, vol 262, pp. 247-261
- Thirumalairajan, S., Girija, K., Hebalkar, N. Y., Mangalaraj, D., Viswanathan, C. and Ponpandian, N. (2013). "Shape Evolution of Perovskite LaFeO<sub>3</sub> Nanostructures: A Systematic Investigation of Growth Mechanism, Properties and Morphology Dependent Photocatalytic Activities". *RSC Adv.*, vol.3, pp. 7549-7561